Available online at www.sciencedirect.com
SCIENCE DIRECT®
Biochimica et Biophysica Acta 1661 (2004) 166–177
BIOCHIMICA ET BIOPHYSICA ACTA
BBA
www.bba-direct.com

Characterization of diphtheria toxin's catalytic domain interaction with lipid membranes

Christian Wolff[a,1], Ruddy Wattiez[b], Jean-Marie Ruysschaert[a], Véronique Cabiaux[a,*]

[a] *Structure et Fonction des Membranes Biologiques, CP 206/2, Université Libre de Bruxelles, Boulevard du Triomphe, B-1050 Brussels, Belgium*
[b] *Service de Chimie Biologique, Université de Mons-Hainaut, Avenue du Champ de Mars 6, 7000 Mons, Belgium*

Received 8 August 2003; received in revised form 19 December 2003; accepted 5 January 2004

Abstract

In response to a low environmental pH and with the help of the B fragment (DTB) the catalytic domain of diphtheria toxin (DTA) crosses the endosomal membrane to inhibit protein synthesis. In this study, we investigated the interaction of DTA with lipid membranes by biochemical and biophysical approaches. Data obtained from proteinase K and trypsin digestion experiments of membrane-inserted DTA suggested that residues 134–157 may adopt a transmembrane orientation and residues 77–100 could be membrane-associated, adopting either a surface or a transmembrane orientation. Fourier transform infrared spectroscopy analysis (FTIR) was used to characterize the secondary and tertiary structure of DTA along its pathway, from the native secreted form at pH 7.2 to the refolded structure at neutral pH after interaction with and desorption from a lipid membrane. We found that the association of DTA with lipid membranes at low pH was characterized by an increase of β-sheet structures and that the refolded structure at neutral pH after interaction with the membrane was identical to the native structure at the same pH. We also investigated the desorption of DTA from the membrane at neutral pH as a function of temperature. Although a complete desorption was observed at 37 °C, no desorption took place at 4 °C. A model of translocation involving the possibility that DTA might insert one or several transient transmembrane domains during translocation is discussed.

Keywords: Diphtheria toxin; Topology; Membrane; Structure; Translocation

1. Introduction

Diphtheria toxin (DT) is secreted as a single polypeptide of 58 kDa by pathogenic strains of *Corynebacterium diphtheriae*. The protein has been crystallized as a monomer and its X-ray structure determined to a 2.3 Å resolution [1]. DT is composed of two subunits: the A chain (DTA or C domain, 21 kDa), which carries the enzymatic activity, and the B chain (DTB, 37 kDa), which contains the translocation domain (T domain) and the receptor binding domain (R domain) [1]. These two fragments are linked by a disulfide bridge in the active form of diphtheria toxin. DT enters the eukaryotic cell by receptor-mediated endocytosis after binding to a specific cell surface receptor, which has been identified as a heparin-binding EGF-like growth factor precursor [2]. The low pH in the endosomes induces a conformational change of the protein that enables DT to leave its receptor [3] and to interact with the endosomal membrane [4–7]. The deep insertion of the DTB domain into the lipid bilayer facilitates the translocation of the catalytic domain to the cytosolic side of the membrane. After reduction of the disulfide bridge, DTA is released into the cytosol where it inhibits protein synthesis by ADP-ribosylation of elongation factor 2 [8,9].

The translocation step, which involves the transport of the catalytic domain through the membrane of early endosomes [10], remains the least understood step in DT cytotoxic pathway. Both DTA and DTB have been shown to deeply interact with the hydrophobic core of the membrane [11–13]. The mechanism of interaction of DTB with the lipid membrane (structure, topology, etc.) has been highly characterized [14–22], and it involves several helices of the T domain of DTB (TH1, TH5-7, TH8-9). Insertion of TH8 and TH9 results in the formation of a cation selective channel [14]. Much less is known about the process by which DTA crosses the endosomal membrane. Recent electrophysiology experiments showed that the T domain

* Corresponding author. Tel.: +32-2-650-5365; fax: +32-2-650-5382.
E-mail address: vcabiaux@ulb.ac.be (V. Cabiaux).
[1] Current address: UCB Pharma, Chemin du Foriest R4, 1420 Braine l'Alleud, Belgium.

0005-2736/$ - see front matter © 2004 Elsevier B.V. All rights reserved.
doi:10.1016/j.bbamem.2004.01.001

is able to translocate the entire catalytic domain (DTA) across planar lipid membranes, which suggests that no other parts of the toxin or cellular proteins are required for this process [23]. At low pH, the A chain undergoes a reversible conformational change in which it partly unfolds and becomes hydrophobic. This unfolding is essential for efficient translocation to occur [24,25]. Insertion of DTA in the lipid membrane has been elegantly characterized by D'Silva and Lala [13]. The full-length DTA protein was inserted into lipid vesicles containing a photoactive and radiolabelled probe (^{3}H diazofluorene). By a combination of chemical cleavages and microsequencing steps, several labelled residues were identified and were then demonstrated to be in interaction with the membrane. As far as the A fragment is concerned, two regions were labelled: between residues 77 and 115 and all the residues extending between Val 134 and Ala 141.

The approach that we previously developed to characterize the topology of DT combines the proteolysis of DT inserted in a lipid membrane and the structure determination by infrared spectroscopy [18]. In addition to several domains of DTB, residues 122 to about 170 of DTA were protected from proteolysis, most probably because of their interaction with the membrane. However, in these experiments, the concentration of the protected DTA peptide was much lower than the protected peptides arising from the B fragment [18] and it was extremely difficult to characterize the structures specifically associated to DTA.

In this paper, we therefore used the isolated catalytic domain of DT in order to investigate more specifically the domains and structures of DTA involved in membrane interaction. DTA was inserted into a lipid membrane and proteolyzed either with proteinase K or trypsin. The protected peptides were purified, identified and their structure was characterized by Fourier transform infrared spectroscopy (FTIR). We also investigated the reversal of DTA-membrane binding. Our results suggest that in addition to the T domain of DTB, specific regions of DTA might play an active role in the translocation process. A model in which DTA may insert one or several transient transmembrane anchors while large domains are translocated across the membrane is discussed.

2. Materials and methods

2.1. Materials

Proteinase K, trypsin (TPCK treated) and asolectin (mixed soybean phospholipid) were from Sigma Chemical Co. (St. Louis, MO). Phenylmethylsulfonylfluoride (PMSF) was from Serva. Polyvinylidene difluoride (PVDF) (problott) membranes were obtained from Applied Biosystems and acrylamide was from Biorad. The *E. coli* strain BL-21 pET-15b was kindly provided by Dr. R.J. Collier (Harvard Medical School, Boston, MA). All other reagents and products were of the highest purity.

2.2. DTA purification

The catalytic domain of DT (DTA) was purified from the *E. coli* strain BL-21 containing the plasmid pET-15b which was kindly provided by Dr. John Collier (Harvard Medical School, Boston). This plasmid encodes DTA carrying an additional N-terminal His-tag (6 His) and a cleavage site for thrombin between the tag and the protein. The protein was expressed and purified according to the procedure of Weiss et al. [26] and stored at −20 °C in a 20 mM Tris–HCl pH 7.2, 150 mM NaCl, 1 mM β-mercaptoethanol buffer.

2.3. Reconstitution of DTA into lipid vesicles

Large unilamellar vesicles (LUV) of asolectin were prepared in a 20 mM Tris–HCl buffer, pH 7.2, 150 mM NaCl as previously described [18]. DTA was mixed with lipid vesicles in the same buffer at a lipid to protein ratio of 8 (w/w) and incubated for 1 h at 37 °C. The pH was then lowered to 5 by addition of a 1 M sodium acetate/acetic acid buffer, pH 5.0 at a final concentration of 100 mM. After 1 h of incubation at 37 °C, the sample was mixed with an equal volume of sucrose 80% (w/v), and overlaid with a 30–2% linear sucrose gradient. The sucrose solutions were prepared in a 20 mM sodium acetate/acetic acid buffer, pH 5, 150 mM NaCl. An overnight centrifugation at 100 000 × *g* in a Beckmann Optima LE-80K ultracentrifuge with a SW 60 rotor allowed the separation of soluble DTA from lipid-bound DTA [27]. The band formed by the liposomes containing DTA was collected. To eliminate the sucrose, the proteoliposomes were pelleted twice in a 20 mM sodium acetate/acetic acid buffer, pH 5, 150 mM NaCl, by centrifugation at 100 000 × *g* for 30 min. The pellet was eventually suspended in 50 μl of the same buffer. The concentration of DTA associated with liposomes was determined according to Lowry et al. [28].

2.4. Proteolysis study

Proteinase K and trypsin were added, respectively, at a 2% or 20% (w/w) protease/DTA ratio to DTA proteoliposomes, prepared as described above, and the sample was incubated at 37 °C. For the digestion kinetics, 50 μl aliquots were removed after various incubation times and the reaction was stopped on ice by adding PMSF at a final concentration of 1 mM for proteinase K and 5 mM for trypsin. The desorbed peptides and the protease were subsequently eliminated by centrifugation on a 30–2% linear sucrose density gradient. The isolated proteoliposomes were washed by a centrifugation step at 100 000 × *g* and suspended in 50 μl of a 20 mM sodium acetate/acetic acid buffer, pH 5.0, 150 mM NaCl. A chloroform/methanol (1:1) extraction [29] allowed the separa-

tion of lipids (in the organic phase) and peptides (in the aqueous phase and at the interface). The recovered peptides were concentrated under a nitrogen flux and separated on a Tris-Tricine-SDS-polyacrylamide electrophoresis gel (16.5% combined acrylamide and bisacrylamide (T), 6% of which is cross-linker (bisacrylamide; C)) [30]. After migration, the peptides were electrotransferred onto a PVDF membrane and stained with Coomassie blue. The peptide bands were cut off the membrane, and the peptides N-terminal sequences were determined by automated Edman degradation using a Beckmann LF3400 protein–peptide microsequencer equipped with an on-line Gold 126 micro-gradient HPLC system and a Model 168 Diode Array detector (Beckmann Instruments, Inc., Fullertown, CA) as described in Quertenmont et al. [18].

For attenuated total reflection (ATR)-FTIR experiments involving proteinase K digested samples, DTA and asolectin vesicles were mixed in a lipid to protein ratio of 2 (w/w) and the original Tris buffer was exchanged by dialysis for a 2 mM Hepes buffer, pH 7.2, 150 mM NaCl, prior to reconstitution. The pH was then lowered to 5 with diluted HCl and the proteolysis was performed as described above. The digested sample (~ 300 μl) was diluted in 4 ml of water adjusted to pH 5.0 with a 60 mM KH_2PO_4 stock solution and the membrane-associated peptides were pelleted by centrifugation. The sample was eventually suspended in 50 μl of water adjusted to pH 5.0 with the 60 mM KH_2PO_4 stock solution and spread at the surface of a germanium plate under N_2 flux. Trypsin digested samples were not analyzed by FTIR since proteolysis most probably leads to a modification of the protein structure which cannot be related to any step of interaction of DTA with a lipid membrane.

2.5. Attenuated total reflection-Fourier transform infrared spectroscopy

ATR infrared spectra (resolution 4 cm^{-1}) were recorded with a Perkin-Elmer 1720X FTIR spectrophotometer as previously described [31]. Measurements and sample deuteration (2 h) were carried out as described in Wang et al. [32]: hydrogen/deuterium (H/D) exchange allows differentiation of the α-helix from the random structure, which absorbance bands shift from about 1655 to about 1642 cm^{-1} [33,34]. The determination of the secondary structure of proteins was carried out by analysis of the deuterated amide I region (1600–1700 cm^{-1}) as previously described [35]. The frequency limits for the different structures were as follows: 1662–1645 cm^{-1}, α-helix; 1689–1682 cm^{-1} and 1637–1613 cm^{-1}, β-sheet; 1645–1637 cm^{-1} (random coil) and 1682–1662 cm^{-1} (β-turns) are referred as random structures. The control spectra of the 2 mM Hepes buffer, pH 7.2, and asolectin vesicles at both pH 7.2 and 5.0 showed no absorbance between 1700 and 1600 cm^{-1} (data not shown). All the samples are spread at the surface of a germanium plate under N_2 flux. Under these conditions the liquid water is removed and the protein keeps its hydration water [36].

2.6. Kinetics of deuteration

The experimental procedure was carried out at pH 5.0 or 7.2 as previously described [37]. The samples were spread on a germanium plate as described above. The spectra at each time point were the accumulation of 12 scans with a resolution of 4 cm^{-1}. The amide I and II band areas were measured, respectively, between 1702–1596 and 1585–1502 cm^{-1}. The amide II area was divided by the amide I area (in the absence of lipids) or the phospholipid C=O band area (in the presence of lipids) for each spectrum to take into account any change in the total intensity of the spectra during the deuteration process. This ratio, which was expressed between 0% and 100%, was plotted versus deuteration time. The 100% value is defined by the amide II/amide I or the amide II/C=O phospholipid ratio before deuteration, whereas the 0% value corresponds to a zero absorbance in the amide II region as shown in previous studies [38,39].

2.7. Desorption experiments at neutral pH

Proteoliposomes containing DTA were pelleted during 1 h at 100 000 × *g* in a 20 mM sodium acetate/acetic acid pH 5, 150 mM NaCl buffer and suspended in 200 μl of TBS buffer (20 mM Tris–HCl pH 7.2, 150 mM NaCl). The samples were further incubated for 1 h at 37 or 4 °C, adjusted to 40% (w/v) sucrose by means of a 80% (w/v) sucrose solution prepared in TBS buffer and overlaid with a discontinuous 30–2% (w/v) sucrose density gradient prepared in the same buffer. Samples were centrifuged overnight at 35 000 rpm (4 °C) in a Beckman LE-80K ultracentrifuge, fractions were collected and analyzed.

For infrared spectroscopy analysis, the DTA proteoliposomes were suspended in a 2 mM Hepes buffer pH 7.2, incubated for 1 h at 37 or 4 °C and the lipid vesicles were subsequently pelleted at 100 000 × *g* during 30 min. Desorbed DTA at 37 °C was recovered in the supernatant whereas for experiments carried out at 4 °C the pellet was suspended in 2 mM Hepes pH 7.2 buffer.

3. Results

3.1. Topology of DTA in a lipid bilayer at pH 5

Proteinase K and trypsin were chosen to analyze the topology of DTA. Proteinase K is a non-specific protease which cleaves preferentially at the C-terminus of aliphatic and hydrophobic residues and should allow to remove all the extramembrane domains of DTA exposed to the enzyme. Trypsin cleaves specifically at the C-terminus of arginine and lysine residues and should allow to localize the Arg and

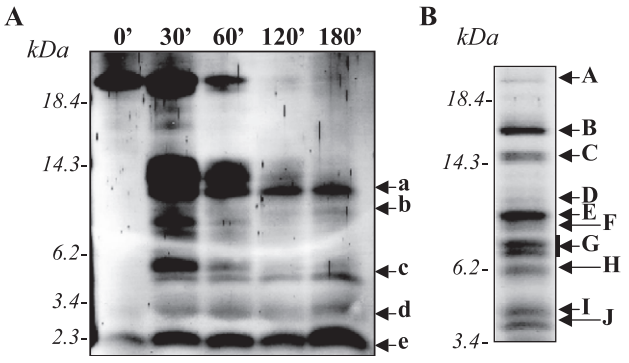

Fig. 1. Proteinase K and trypsin digestion profiles of membrane-inserted DTA at pH 5.0. Silver staining of a Tris-Tricine-SDS-polyacrylamide gel (16.5% T, 6% C). (A) DTA proteoliposomes were treated for various times with 2% (w/w) proteinase K. Time 0′ represents the proteoliposomes before addition of the protease. (B) Digestion profile of membrane-inserted DTA by trypsin at pH 5 after separation on a sucrose density gradient.

Lys residues exposed to the outside of the membrane. The two enzymes are complementary and their combined use should give reliable information about topology. To identify the DTA peptides in interaction with the lipid membrane at pH 5, proteolysis was performed on membrane-inserted DTA either in the presence of 2% (w/w) proteinase K or 20% (w/w) trypsin (see Materials and methods). The reaction was stopped on ice after various incubation times in the presence of PMSF and the digested proteoliposomes were subsequently isolated by centrifugation on a sucrose density gradient. The membrane-associated peptides were freed from lipids by a chloroform/methanol extraction and separated on a Tris-Tricine-SDS-polyacrylamide gel (Fig. 1). In the presence of proteinase K (Fig. 1A), DTA was rapidly cleaved into low molecular weight peptides and the entire protein at 21 kDa completely disappeared after 2 h incubation. A time-stable digestion pattern was obtained after 3 h of proteinase K treatment and gave rise to five major bands:

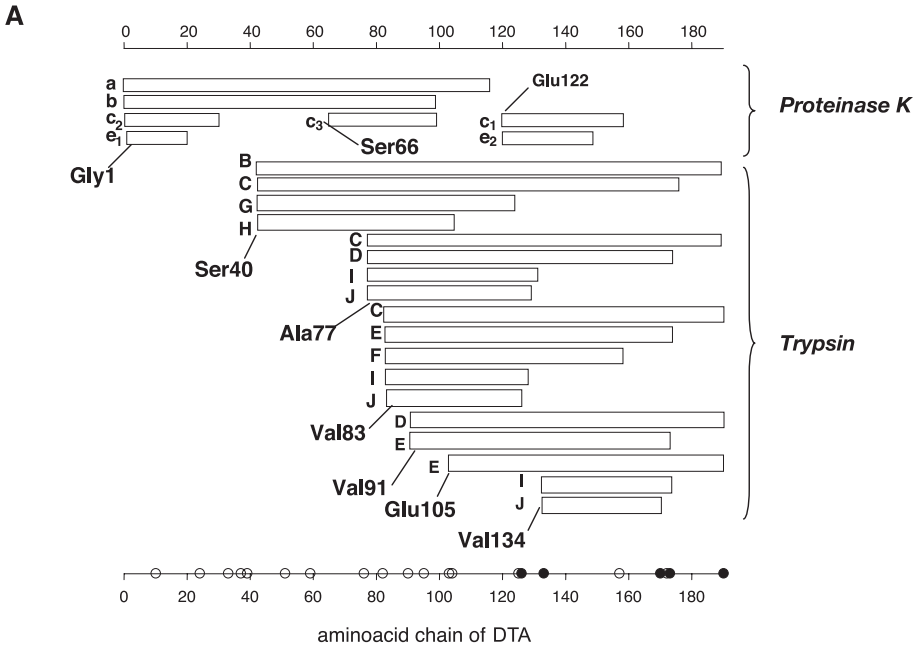

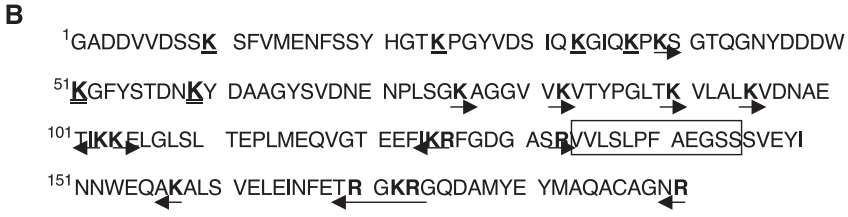

Fig. 2. Location of the DTA-protected peptides generated by proteinase K and trypsin digestion. (A) The protected regions of DTA (cf. bands from Fig. 1) are presented as boxes and their respective N-terminal residues, as determined by microsequencing, are indicated. The C-terminal boundaries of these peptides were estimated according to the apparent molecular weight of the peptide bands on the electrophoresis gel (Fig. 1) and should be considered as approximative. The positions of arginine and lysine residues are indicated by closed and open circles, respectively. (B) Amino acid sequence of DTA. Arginine and lysine residues identified by proteolysis (N- or C-terminus of peptides) are indicated by arrows, cleaved residues are underlined and protected residues are double underlined (Lys51 and Lys59). Region 134–145 is indicated by a box.

band a (~ 13 kDa), band b (~ 11 kDa), band c (~ 4 kDa), band d (~ 3 kDa) and band e (~ 2.4 kDa). Trypsin cleavage of membrane-inserted DTA generated, in addition to a low amount of uncleaved DTA, nine peptide bands (B–J) within the range of 20–4 kDa (Fig. 1B) and about 2 h of incubation were required to obtain a stable trypsin digestion pattern (data not shown). After purification of the digested proteoliposomes on a sucrose density gradient the nine peptide bands (B–J, Fig. 1B) obtained from trypsin digestion and the five peptide bands (a–e, Fig. 1A) resulting from proteinase K cleavage were transferred from an unstained electrophoresis gel onto a PVDF membrane, excised from the membrane, and their N-terminal amino acid sequences were determined by microsequencing. The position of each peptide within the amino acid chain of DTA is presented in Fig. 2.

From the five bands obtained by proteinase K treatment, seven different peptide sequences were identified (Table 1): bands a and b contained single peptides extending from the N-terminal end of DTA towards approximately residue 120 or 100, respectively. Band c was found to contain three peptides: the first extended from Glu122 to about residue 160 (c_1), the second peptide covered approximately the first 30 amino acids (c_2) and the third peptide was calculated to extend between Ser66 and approximately residue 100 (c_3). For band d, no identifiable amino acid derivates could be determined, which suggests that this band might result from a staining artifact. Band e contained two small peptides located, respectively, between residues 1–20 (e_1) and 122–145 (e_2). Only three different N-terminal boundaries were identified for the seven sequenced peptides, located respectively at Gly1 (peptides a, b, c_2, e_1), Ser66 (peptide c_3) and Glu122 (peptide c_1, e_2). The identification of four different peptides within the N-terminal region of DTA, all starting at Gly1 (peptides a, b, c_2, e_1), suggests that approximatively the first 20 or 30 amino acids remain inaccessible to the protease. Similarly, residues 66 to about 100 and 122 to about 160 would also be resistant to enzymatic cleavage.

Trypsin digestion of membrane-inserted DTA yielded 18 different peptides (Table 1). According to the N-terminal sequences, all the peptides were generated from the cleavage of one of the following six residues (Fig. 2B, right arrow): Lys39, Lys76, Lys82, Lys90, Lys104 and Arg133. The C-terminal boundaries of these peptides, which consequently should correspond to either an arginine or lysine residue, were estimated according to their apparent molecular weight on the electrophoresis gel and corresponded to residues 103, 125–126, 157 and 170–173 (left arrow), thus indicating that all these residues are exposed to the outside of the membrane. No peptide was identified between Gly1 and Lys 39, suggesting that this region has been completely hydrolyzed at either of the four lysine residues (Lys10, Lys24, Lys33, Lys37) leading to peptides too small to be identified under our experimental conditions (less than 1.5 kDa). In particular, Lys 10 must be exposed because its protection would have lead to a peptide of at least 2.5–3 kDa, detectable on a Tris-Tricine gel. No cleavage sites were identified at Lys51 and Lys59 (cf. peptides starting at Ser40), suggesting that these two residues are protected or, at least, much less accessible than the other Arg/Lys residues. The proteolysis results will be discussed in terms of topology and mechanism of translocation in the discussion section.

Table 1
N-terminal amino acid sequences of DTA membrane-associated peptides generated by trypsin and proteinase K digestion

Peptide band	N-terminal sequence	Apparent molecular weight (kDa)
B	^{40}SGTQGNYDDD	15.8
C	^{77}AGGVVKVTYPG	13.7
	^{40}SGTQGNYDD	
	^{83}VTYPGLTKVLA	
D	^{77}AGGVVKVTYP	10.9
	^{91}VLALKVDNAET	
E	^{105}ELGLSLTEPLME	9.8
	^{83}VTYPGLTKVLA	
	^{91}VLALKVDNAET	
F	^{83}VXYPGLTK	9.1
G	^{40}SGTQGNYDD	8.2
H	^{40}SGTQGNY	7.0
I	^{77}AGGVVLV	5.0
	^{83}VTYPGLTK	
	^{134}VVLSLPFAEG	
J	^{134}VVLSLPFAEG	4.4
	^{77}AGGVVLV	
	^{83}VTYPGLTK	
a	^{1}GADDVVDSSKS	13
b	^{1}GADDVVDSSK	11
c_1	^{122}EFIKRFGDGA	4
c_2	^{1}GADDVVDSS	
c_3	^{66}SVNENPLSG	
d	no residues identified	3
e_1	^{1}GADDVVDSSKSF	2.4
e_2	^{122}EFIKRFGDGA	

The letters in the first column correspond to the peptide bands observed in Fig. 1. The approximative C-terminal boundaries of the peptides were estimated on the basis of their apparent molecular weight on the electrophoresis gel.

3.2. Secondary structure of DTA in a lipid membrane at pH 5

The FTIR method is based on the analysis of the vibration bands of protein and particularly the amide I band, ν(C=O) of the peptide bond (1700–1600 cm^{-1}), whose frequency of absorbance is strongly dependent upon the secondary structure. This method has been successfully used to investigate the structure of soluble and membrane proteins [37,40–44]. Since the structural changes affecting the DT catalytic domain during translocation are not well understood, the purpose of this study was to investigate in more detail the secondary structure changes affecting DTA during membrane interaction at low pH.

Fig. 3 shows the FTIR spectra of deuterated DTA at pH 5 in the absence and presence of lipid vesicles, before and after digestion by proteinase K. In the absence of lipids (Fig. 3a), the amide I band of DTA shows a maximum of absorption around 1642 cm^{-1}, indicating that the protein under these conditions presents a high degree of irregular structures which is consistent with all published data of DTA structure at low pH. A curve-fitting procedure [35] enabled us to estimate that in the absence of lipids DTA contained $25 \pm 5\%$ α-helix, $27 \pm 5\%$ β-sheet, $20 \pm 5\%$ random coil and $28 \pm 5\%$ β-turn structures (see Materials and methods). The presence of asolectin vesicles (Fig. 3b) induces a drastic change in the shape of the DTA amide I band and results in a shift of its absorption maximum from 1642 to 1622 cm^{-1}. To estimate the nature of the secondary structures involved in this conformational change, we subtracted the spectrum of DTA obtained in the absence of lipids from the membrane-inserted protein spectrum (Fig. 3b–a). The difference spectrum shows that during membrane interaction, DTA increases its content in β-sheet structures (positive peak at ~ 1620 cm^{-1}) concomitantly with a loss of random coil and β-turn structures (negative peaks respectively at ~ 1640 and ~ 1665 cm^{-1}). The secondary structure analysis agrees with this observation since we determined that membrane interaction results in a significant increase of 26% in β-sheet structures and a loss of about 18% in β-turn structures (Fig. 3). The variation of the content in α-helix and random coil structures lies within the expected experimental error of $\pm 5\%$ and we were therefore unable to determine whether these structures were significantly affected during the conformational change.

To investigate the structure of the membrane-associated peptides of DTA, proteoliposomes containing DTA were prepared and treated with proteinase K (as described in Materials and methods) and spread at the surface of a germanium plate. The amide I band of the deuterated spectrum (Fig. 3c) shows a maximum of absorption around 1626 cm^{-1}, indicating that the membrane-associated peptides contained predominantly β-sheet structures. The curve-fitting analysis gave 46% β-sheet structures, 20% of random and 20% of α-helical structures These results suggest that membrane interaction of DTA might be predominantly triggered by β-sheet structures.

To further characterize the conformational changes taking place upon lipid binding and insertion, we measured the kinetics of deuteration of DTA in the absence and presence

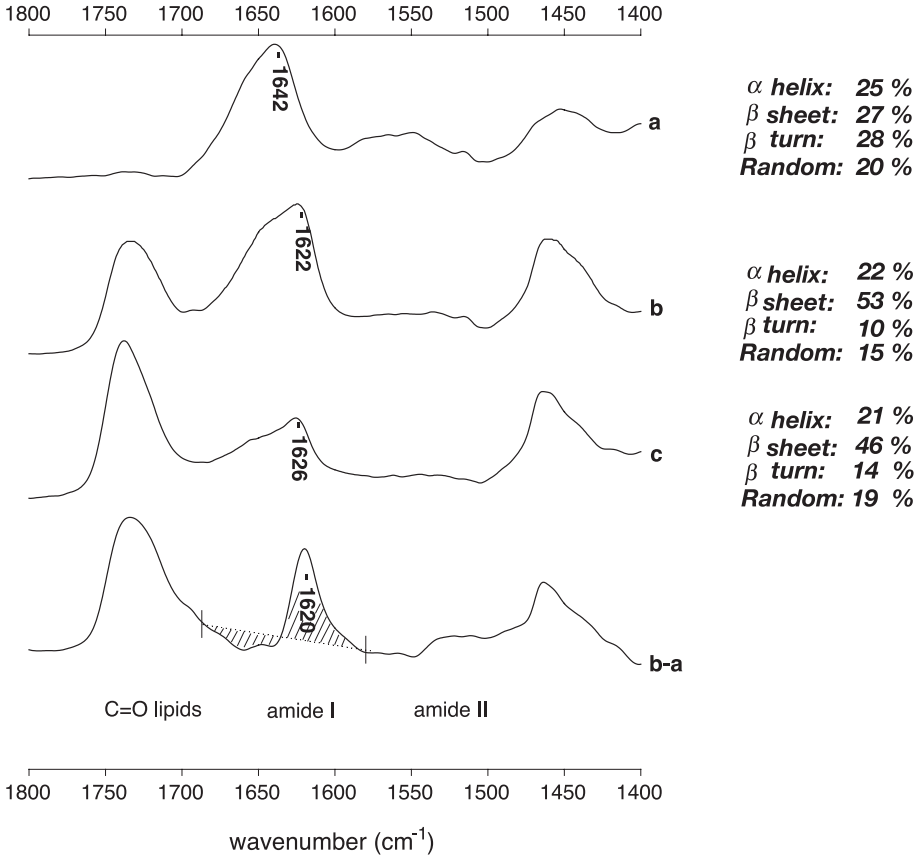

Fig. 3. Infrared spectra of deuterated DTA at pH 5.0 (a) in the absence of lipids, (b) associated to asolectin vesicles before and (c) after digestion by proteinase K. Spectrum (b–a) represents the difference of the corresponding spectra and a subtraction factor of 1.7 was chosen in order to zero the area of the amide I region. Spectrum c was enlarged by a factor of 1.3 compared to spectrum b. The region between 1700 and 1770 cm^{-1} corresponds to the $\nu_{C=O}$ vibration band of the lipids and the region between 1600 and 1700 cm^{-1} corresponds to the $\nu_{C=O}$ vibration band (amide I) of the protein. The spectra intensities have been rescaled for better comparison.

of lipids, before and after proteinase K treatment. The accessibility of the NH amide groups of the protein to the solvent could be measured by exchanging the amide hydrogens of the sample with a D_2O saturated N_2 flux [37]. The peptide hydrogen exchange of the protein was followed by monitoring the decrease of the amide II absorbance peak [δ(N–H) in the 1596–1502 cm^{-1} region], which is shifted to the 1460 cm^{-1} region [amide II′, δ(N–D)] upon deuteration. The percentage of non-exchanged residues at each time point was calculated from the ratio of amide II/amide I (in the absence of lipids) or amide II/C=O lipids areas (in the presence of lipids).

Fig. 4 shows the H/D exchange kinetics at pH 5 of free or membrane-inserted DTA, before and after proteinase K treatment. In the absence of lipids, DTA undergoes a very fast exchange as already 50% of the residues were exchanged after only 3 min. This deuteration kinetic reaches a stable value of 35% of non-exchanged residues after 100 min, indicating that under these conditions about 67 amino acids of DTA (35% of 190 residues) are not accessible to the solvent and thus most probably buried inside of the protein. This suggests that although DTA is partially denaturated by the pH, not all residues are easily exchangeable. In the presence of asolectin vesicles, the evolution of the kinetic is much slower and about 40 min are needed to exchange 50% of the residues. The decrease of the exchange rate most probably results from the conversion of unordered structures into β-sheet observed upon membrane interaction since it has been shown that the amide groups of β-sheet structures

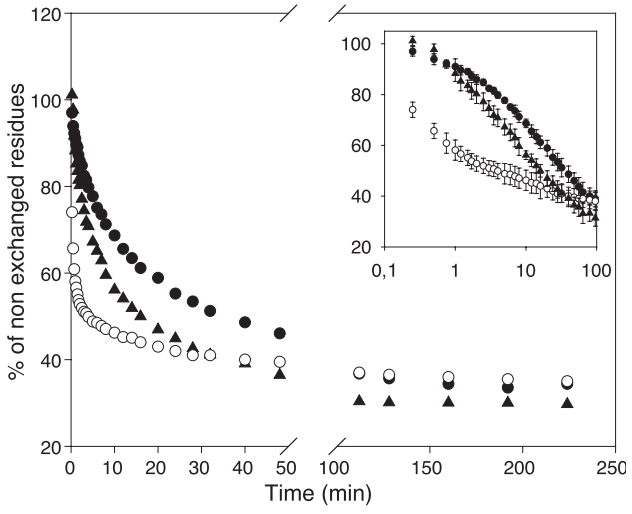

Fig. 4. H/D exchange kinetics of DTA at pH5. The evolution of the proportion of non-exchanged residues as a function of deuteration time is shown for DTA at pH 5.0 either in the absence of lipids (○) or associated to asolectin vesicles before (●) or after proteinase K treatment (▲). The amide II/amide I area ratio (○) or the amide II/C=O lipid area ratio (●; ▲) for each spectrum, which was expressed between 0% and 100%, was reported as a function of deuteration time. Insert: early time points are presented on a logarithmic scale. Each curve is the average of three independent experiments, and the error bars represent the standard deviation.

exchange a 1000-fold slower than unordered coil structures [45]. Nevertheless, extensive deuteration (120 min) shows that membrane-inserted DTA exchanges to the same level as the soluble protein (35% of non-exchanged residues) indicating that membrane interaction does not affect the overall accessibility of the protein. These results suggest that either a very low number of residues are protected by the lipid membrane, in addition to those which are buried in the soluble protein, or that a similar number of residues that are buried in the soluble protein because of the folding are now protected from the solvent because of their insertion in the lipid membrane.

After proteinase K treatment, DTA shows a faster exchange than the one observed for the non-digested sample. These results indicate that at least a part of the slow exchanging structures such as β-sheets have been eliminated during proteolysis and suggest that these structures are also located within extramembrane domains of DTA.

3.3. Characterization of the desorption process of DTA from a lipid membrane at neutral pH

The binding of DTA to a lipid membrane has been shown to be fully reversible upon exposure to neutral pH [11,46]. This process is of major importance in vivo since after translocation across the endosomal membrane, DTA has to refold in the cytosol to express its cytotoxic activity. The implication of cellular proteins, such as chaperones, in the refolding process of DTA is still a matter of debate. To get a better understanding of the refolding mechanism of DTA, we investigated the dissociation of DTA from the lipid membrane at neutral pH. Although our approach does not represent the system after translocation across the cellular membrane, it still should allow to obtain structural information about the reversal of the DTA conformation once it has interacted with the lipid membrane at low pH.

DTA was inserted into lipid vesicles at pH 5 and the desorption was subsequently induced by exposing the proteoliposomes to neutral pH (see Materials and methods). The membrane-dissociated protein was isolated by centrifugation and its conformation was investigated by FTIR. The spectra of DTA after desorption from the lipid membrane at pH 7.2 is shown in Fig. 5A. The overall shape of the amide I region of desorbed DTA is very similar to the one observed for native DTA at pH 7.2 (Fig. 5A, a–b). Furthermore, the deconvoluted spectra (Fig. 5A, c–d) clearly indicate that in both cases, DTA presents the same secondary structure components, suggesting that dissociation of DTA from the lipid membrane at neutral pH leads to the recovery of the native secondary structures. To investigate whether the folding of desorbed DTA is also compatible with its native tertiary structure, we compared the H/D exchange kinetics of the native and the membrane-desorbed forms of DTA at pH 7.2 (Fig. 5B). The evolution of the H/D exchange for desorbed DTA was identical for the two proteins and we therefore conclude that DTA regains its

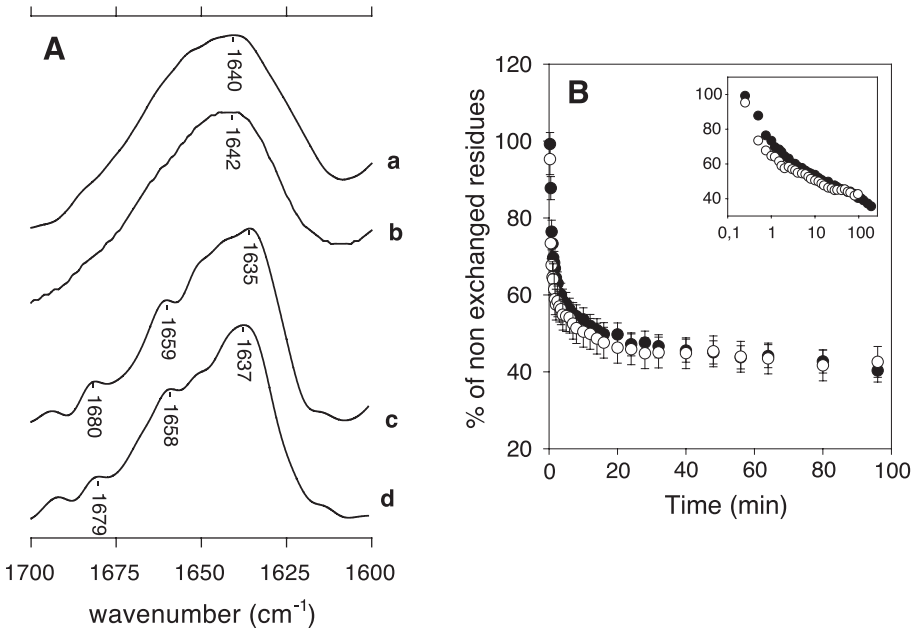

Fig. 5. Structure of DTA after desorption from the lipid membrane at pH 7.2. (A) Amide I region of deuterated native DTA at pH 7.2 (a) or after desorption from the lipid bilayer at pH 7.2 (b). The deconvoluted spectra are shown in (c) and (d), respectively. The spectra intensities have been rescaled for better comparison. (B) H/D exchange kinetic of native DTA (○) or desorbed DTA (●) at pH 7.2. Insert: time points are presented on a logarithmic scale. Error bars represent the standard deviation of three independent experiments.

native secondary and tertiary structures after interaction with a lipid membrane.

To further dissect the dissociation of DTA from the membrane upon exposure to neutral pH, we investigated the desorption process at 4 °C. This temperature should allow us to slow down the redissociation dynamic and thus to trap the protein in an intermediate structural state, if it exists. For this purpose, proteoliposomes containing DTA were pelleted by centrifugation and suspended in a 2 mM Hepes pH 7.2 buffer and incubated during 1 h at 4 or 37 °C. The samples were centrifuged on a sucrose density gradient (pH 7.2, 4 °C) and the fractions were assayed for their content in lipids and proteins (Fig. 6). When the whole experiment was carried out at low temperature, about 70% of DTA remained associated to the lipid membranes, whereas it is almost fully desorbed, as expected, when the first incubation was performed at 37 °C. Infrared spectroscopy analysis showed that the amide I region of the membrane-associated DTA sample incubated at 4 °C (Fig. 7A, b) presents the structural characteristics of both the membrane-associated (Fig. 7A, a) and the membrane-desorbed (Fig. 7A, c) forms. The amide I region is characterized by the presence of two major maxima: one located around 1640 cm^{-1}, which is characteristic for the native form of DTA,

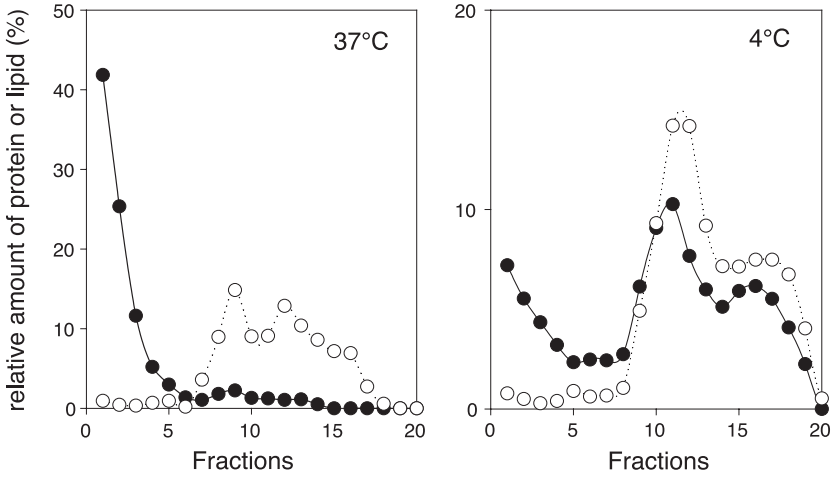

Fig. 6. Desorption of membrane-inserted DTA at pH 7.2 after separation on a continuous 30–2% (w/v) sucrose density gradient. The fractions were collected from the bottom of the tube and the content in protein (●) and lipids (○) were determined, respectively, by tryptophan fluorescence at 330 nm and by a phosphatidylcholine assay (Roche). Data is presented as the percentage of the total amount of protein or lipids detected on the gradient.

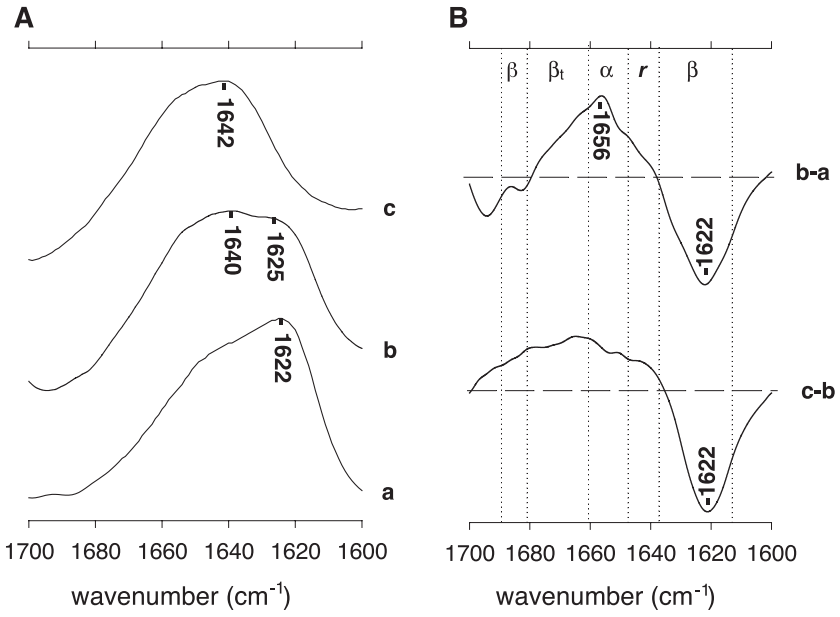

Fig. 7. Evolution of the amide I region of DTA during dissociation from the lipid membrane at neutral pH. (A) Experimental deuterated spectra and (B) difference spectra are shown: (a) membrane-inserted DTA at pH5 (from Fig. 3); (b) membrane-inserted DTA exposed to neutral pH (4 °C); (c) desorbed DTA at pH 7.2 (37 °C). Difference spectra were generated by using subtractions factors of 0.3 and 0.5 for b−a and c−b, respectively, in order to zero the area of the amide I band. The baseline is indicated by a horizontal dotted lines. The difference spectra b−a and c−b were magnified by a factor of 2.5 and 1.5, respectively. Secondary structures limits for alpha helices (α), beta (β), random coil (r) and beta turn (β_t) structures are indicated by vertical dotted lines.

and a second around 1625 cm^{-1} characteristic for the membrane-associated form of DTA. To analyze the secondary structures changes affecting membrane-inserted DTA after exposure to neutral pH at 4 °C the spectrum obtained for membrane-inserted DTA at pH 5, which represents the initial state, was substracted from the spectrum obtained for DTA at neutral pH, 4 °C (termed the intermediate state) (Fig. 7B, b−a). The transition to the intermediate state results in a loss of β-sheet structures (negative peak at 1622 cm^{-1}) and an increase in α-helical and β-turn structures (positive peak). The transition from the intermediate state of DTA to the complete desorbed state (Fig. 7B, c−b) is characterized by a further decrease of the component at 1622 cm^{-1} and an increase of other secondary structures.

The results suggest that DTA could start the refolding of its extramembrane domains before the protein is completely desorbed from the membrane. However, we cannot infer from the data whether DTA is strongly or loosely associated to the membrane when refolding starts. Therefore, how the complete refolding is associated to the desorption from the membrane remains to be elucidated.

4. Discussion

The translocation process of DTA across the endosomal membrane remains one of the least understood steps in DT cytotoxic pathway. The first proposed model was based on the finding that the T domain of DTB was forming a channel in lipid membrane: DTA would cross the membrane in an unfolded form, through the aqueous channel formed by DTB [14]. However, the data showing that DTA was able to directly interact with the membrane have questioned this model. The model that is currently discussed for translocation of DTA is the chaperone model which is based on the observation that membrane-inserted T domain recognizes and binds to hydrophobic, partly unfolded peptides. According to this model, the T domain plays the role of a chaperone for a partly unfolded and hydrophobic form of the A chain. DTA translocates through the membrane, in association with the T domain, via a number of relatively non-specific and transient binding events between the T domain and DTA [47]. To further investigate the DTA translocation process, we identified the regions of isolated DTA in interaction with a lipid membrane and we characterized their structure by FTIR.

The proteolysis experiments on membrane-inserted DTA at pH 5 indicate that some restricted regions of DTA remain specifically protected against externally added proteases and might therefore represent membrane-associated domains (Fig. 8). In the C-terminal region of DTA, res 122 to about 145 and res 134–157[2] were protected, when proteinase K or trypsin were respectively used. A strict overlapping of these two regions indicate that, at least residues 134 to about 145

[2] The C-terminal end evaluations were based on the apparent molecular mass measurement on the electrophoresis gel and should therefore be considered as indicative in the case of proteolysis by proteinase K. It is more accurate in the case of trypsin since the C-terminal residue must be an arginine or a lysine.

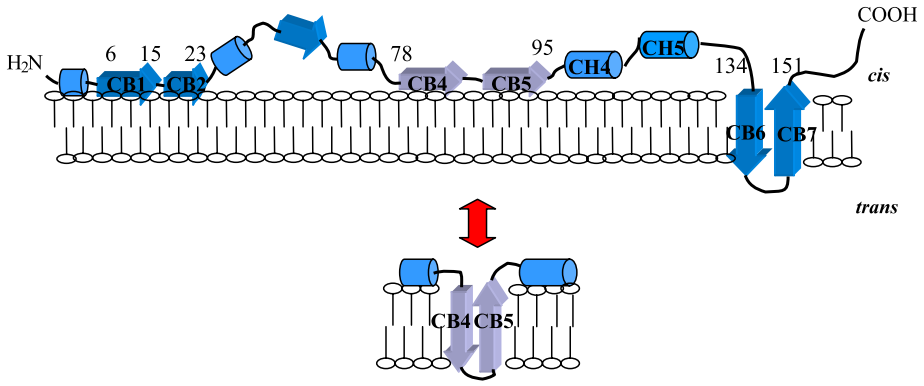

Fig. 8. Topological model of DTA in interaction with a lipid bilayer. The "cis" side is the side of the membrane to which DTA was added; the "trans" side represents the interior of the liposomes. This model does not take into account the interactions between secondary structures nor the interaction with DTB domains. The double arrow indicates the two putative conformations of the central region of DTA, a shallow insertion (above) or a deep membrane insertion (below).

might be inserted in the lipid membrane. This is in excellent agreement with the data of D'Silva and Lala [13] showing that in the full-length protein residues 134–141 were strongly labelled by a membrane probe. According to the crystal structure of DT this particular region of DTA contains a β-hairpin structure (CB6–CB7, residues 133–151) and we therefore suggest that this hairpin could insert as such into the lipid membrane and adopt a transmembrane orientation. Such an orientation is probably also observed in the presence of the B fragment since we already demonstrated that residues 122–170 were protected from digestion when the whole protein was used [18]. A role for the 134–151 region in translocation is supported by the study of Falnes and Olsnes [48] demonstrating that the use of DT mutants containing internal disulfide bridges (C119–C152, C58–C146) within this C-terminal region prevented both the interaction and translocation of DTA across the cell membrane. The presence of disulfide bridges could block the protein in a particular conformation and thus prevent the insertion of the C-terminal β-hairpin structure into the target membrane.

A second region protected from proteinase K digestion is located from residue 66 to about residue 100. According to the crystal structure of DTA [26], this region contains two successive beta strands structures, CB4 and CB5 (residues 78–95). The protected peptide overlaps a region (77–115) which according to D'Silva and Lala [13] is in interaction with the lipid membrane: the authors observed a specific labelling of this peptide region by a membrane probe but they were not able to identify the labelled residues. Taking the data together (labelling and proteolysis), it appears that the interacting region could be restricted to residues 77–100. However, several trypsin-accessible sites (Lys 76, 82, 90) were also identified in the 77–100 region. We therefore suggest that the interaction of the peptide 77–100 is characterized by an equilibrium between a transmembrane and a surface association. The transmembrane form would generate peptide c_3 (proteinase K) and the trypsin-treated peptides starting at residues 40, whereas the surface orientation would generate all the peptides starting at residues 77, 83 and 91. Such an equilibrium has already been suggested for the interaction of several helices of DTB with the lipid membrane [22]. It remains anyway that CB4–CB5 and CB6–CB7 contain several hydrophilic/charged residues which would make the insertion of single pair of β-strands (such as CB6–CB7) in the membrane quite unfavourable. The co-insertion of CB4–CB5 and CB6–CB7 would facilitate shielding of hydrophilic/charged residues away from the membrane interior. On the other hand, if CB4–CB5 do indeed fluctuate from a surface to a transmembrane orientation, insertion of the hydrophilic residues of CB6–CB7 could be facilitated by the oligomerization of the protein. Such an oligomerization is supported by our FTIR analysis of membrane-inserted DTA which indicated the presence of low-frequency beta sheet structures (1626 cm^{-1}), which could be assigned to aggregated β-strands that would be related to the oligomerization of DTA [49,50].

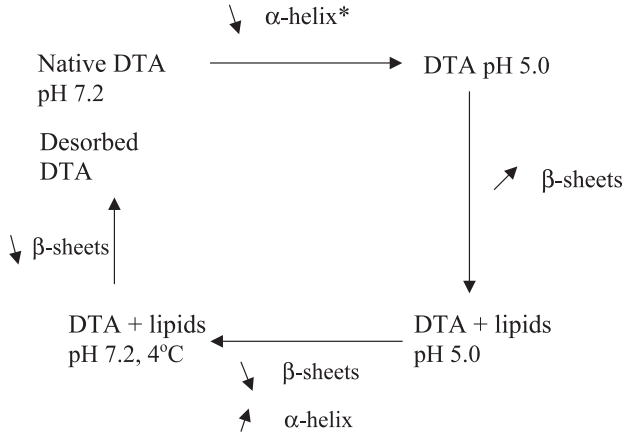

Fig. 9. Conformational changes associated to DTA along its pathway from the outside of the cells (pH 7.2 native form) to the cell cytoplasm (pH 7.2 membrane-released form). Upward and downward arrows indicate, respectively, the relative increase and decrease of the secondary structure content of the protein. (*) The conformational changes from the native DTA at pH 7.2 to DTA at pH 5.0 were investigated in Cabiaux et al. [35].

Region 40–66 contains two non-hydrolyzed lysines but is completely digested by proteinase K, suggesting that the lysine protection might result from a local protein secondary structure rather than from the interaction with the membrane.

The topology of the N-terminal region of DTA (residues 1–40) is more difficult to interpret. It is protected against proteinase K but entirely accessible to trypsin. This specific region contains two β-strand structures (CB1 6–15 and CB2 17–23), which could interact with the surface of the membrane, with the hydrophobic residues inserted in the lipid membrane and thus inaccessible to proteinase K, whereas lysine residues would face the solvent, remaining accessible to trypsin.

To summarize, three regions putatively in interaction with the lipid membrane were identified:

- Region 134–151, containing CB6–CB7, with a transmembrane orientation.
- Region 78–95, containing CB4–CB5, which could adopt both a surface and a transmembrane orientation.
- Region 1–23 which could associate to the surface of the lipid membrane.

This strongly suggests that DTA might be able to insert into the lipid membrane one or several transient transmembrane domains, characterized by a β-sheet structure, in agreement with our FTIR data showing that interaction with the membrane is mostly triggered by β-sheets (Fig. 9). The presence of at least one transmembrane anchor is supported by our data showing that DTA remains mostly associated to the membrane at neutral pH, at low temperature whereas it is desorbed at 37 °C. How the long hydrophilic domains between the transmembrane anchors are translocated cannot be inferred from our experiments. It is however conceivable that they could cross the membrane through a "channel-like" structure formed by both DTA and DTB regions in interaction in the lipid membrane. How this "channel-like" structure is related to the well-characterized TH8–TH9 channel remains to be elucidated. The structural characterization of the membrane-associated form of DTA at neutral pH and low temperature is giving some insight about how the membrane anchor(s) could eventually be desorbed from the membrane (Fig. 9): the intermediate state trapped at pH 7.2 and 4 °C is characterized by an increase of the α-helical structure suggesting that the protein can start its refolding while still bound to the membrane. This "initial" refolding could then induce the desorption of the membrane anchor(s) to go back to the native structure.

The translocation of toxins across the cell membrane is a very complex mechanism and it is particularly difficult to address the question of the dynamics of translocation. We suggest here that DTA, in addition to transient binding to DTB, as suggested by the chaperone model, might insert transient transmembrane domains into the membrane, allowing the translocation, of the main part of its sequence. The transmembrane domain(s) would then be desorbed, perhaps as a consequence of the refolding at pH 7.2 of the translocated region. Further structural and topological characterization will be required to confirm this hypothesis.

Acknowledgements

This work was supported by the Fonds pour la Recherche dans l'Industrie et l'Agriculture (FRIA, Belgium) and by the Ministère de l'Education Nationale et de la Formation Professionnelle (Luxemburg). R.W. and V.C. are respectively research associate and senior research associate of the National Fund for Scientific Research.

References

[1] M.J. Bennett, D. Eisenberg, Domain swapping: entangling alliances between proteins, Protein Sci. 3 (1994) 1464–1475.
[2] J.G. Naglich, J.E. Metherall, D.W. Russell, L. Eidels, Expression cloning of a diphtheria toxin receptor: identity with a heparin-binding EGF-like growth factor precursor, Cell 69 (1992) 1051–1061.
[3] J.S. Brooke, J.H. Cha, L. Eidels, Diphtheria toxin receptor interaction: association, dissociation, and effect of pH, Biochem. Biophys. Res. Commun. 248 (1998) 297–302.
[4] K. Sandvig, S. Olsnes, Diphtheria toxin entry into cells is facilitated by low pH, J. Cell Biol. 87 (1980) 828–832.
[5] K. Sandvig, S. Olsnes, Rapid entry of nicked diphtheria toxin into cells at low pH. Characterization of the entry process and effects of low pH on the toxin molecule, J. Biol. Chem. 256 (1989) 9068–9076.
[6] M.G. Blewitt, L.A. Chung, E. London, Effect of pH on the conformation of diphtheria toxin and its implications for membrane penetration, Biochemistry 24 (1985) 5458–5464.
[7] Q.F. Defrise, V. Cabiaux, M. Vandenbranden, R. Wattiez, P. Falmagne, J.M. Ruysschaert, pH-dependent bilayer destabilization and fusion of phospholipidic large unilamellar vesicles induced by diphtheria toxin and its fragments A and B, Biochemistry 28 (1989) 3406–3413.
[8] J. Pappenheimer-AM, Diphtheria toxin, Ann. Rev. Biochem. 46 (1977) 69–94.
[9] R.J. Collier, Effect of diphtheria toxin on protein synthesis: inactivation of one of the transfer factors, J. Mol. Biol. 25 (1967) 83–98.
[10] E. Lemichez, M. Bomsel, G. Devilliers, J. vanderSpek, J.R. Murphy, E.V. Lukianov, S. Olsnes, P. Boquet, Membrane translocation of diphtheria toxin fragment A exploits early to late endosome trafficking machinery, Mol. Microbiol. 23 (1997) 445–457.
[11] C. Montecucco, G. Schiavo, M. Tomasi, pH dependence of the phospholipid interaction of diphtheria-toxin fragments, Biochem. J. 231 (1985) 123–128.
[12] J.O. Moskaug, H. Stenmark, S. Olsnes, Insertion of diphtheria toxin B-fragment into the plasma membrane at low pH, J. Biol. Chem. 266 (1991) 2652–2659.
[13] P.R. D'Silva, A.K. Lala, Organization of diphtheria toxin in membranes, J. Biol. Chem. 275 (2000) 11771–11777.
[14] B.L. Kagan, A. Finkelstein, M. Colombini, Diphtheria toxin fragment forms large pores in phospholipid bilayer membranes, Proc. Natl. Acad. Sci. U. S. A. 78 (1981) 4950–4954.
[15] K. Sandvig, S. Olsnes, Diphtheria toxin-induced channels in Vero cells selective for monovalent cations, J. Biol. Chem. 263 (1988) 12352–12359.
[16] P.O. Falnes, I.H. Madshus, K. Sandvig, S. Olsnes, Replacement of negative by positive charges in the presumed membrane-inserted

part of diphtheria toxin B fragment. Effect on membrane translocation and on formation of cation channels, J. Biol. Chem. 267 (1992) 12284–12290.
[17] I.H. Madshus, The N-terminal alpha-helix of fragment B of diphtheria toxin promotes translocation of fragment A into the cytoplasm of eukaryotic cells, J. Biol. Chem. 269 (1994) 17723–17729.
[18] P. Quertenmont, R. Wattiez, P. Falmagne, J.M. Ruysschaert, V. Cabiaux, Topology of diphtheria toxin in lipid vesicle membranes: a proteolysis study, Mol. Microbiol. 21 (1996) 1283–1296.
[19] S.E. Malenbaum, R.J. Collier, E. London, Membrane topography of the T domain of diphtheria toxin probed with single tryptophan mutants, Biochemistry 37 (1998) 17915–17922.
[20] Y. Wang, S.E. Malenbaum, K. Kachel, H. Zhan, R.J. Collier, E. London, Identification of shallow and deep membrane-penetrating forms of diphtheria toxin T domain that are regulated by protein concentration and bilayer width, J. Biol. Chem. 272 (1997) 25091–25098.
[21] J. Ren, J.C. Sharpe, R.J. Collier, E. London, Membrane translocation of charged residues at the tips of hydrophobic helices in the T domain of diphtheria toxin, Biochemistry 38 (1999) 976–984.
[22] M.P. Rosconi, E. London, Topography of helices 5–7 in membrane-inserted diphtheria toxin T domain: identification and insertion boundaries of two hydrophobic sequences that do not form a stable transmembrane hairpin, J. Biol. Chem. 277 (2002) 16517–16524.
[23] K.J. Oh, L. Senzel, R.J. Collier, A. Finkelstein, Translocation of the catalytic domain of diphtheria toxin across planar phospholipid bilayers by its own T domain, Proc. Natl. Acad. Sci. U. S. A. 96 (1999) 8467–8470.
[24] J.X. Jiang, F.S. Abrams, E. London, Folding changes in membrane-inserted diphtheria toxin that may play important roles in its translocation, Biochemistry 30 (1991) 3857–3864.
[25] P.O. Falnes, S. Choe, I.H. Madshus, B.A. Wilson, S. Olsnes, Inhibition of membrane translocation of diphtheria toxin A-fragment by internal disulfide bridges, J. Biol. Chem. 269 (1994) 8402–8407.
[26] M.S. Weiss, S.R. Blanke, R.J. Collier, D. Eisenberg, Structure of the isolated catalytic domain of diphtheria toxin, Biochemistry 34 (1995) 773–781.
[27] V. Cabiaux, P. Quertenmont, K. Conrath, R. Brasseur, C. Capiau, J.M. Ruysschaert, Topology of diphtheria toxin B fragment inserted in lipid vesicles, Mol. Microbiol. 11 (1994) 43–50.
[28] S. Lowry, N.J. Rosebrough, A.L. Farr, R.J. Randall, Protein measurements with the folin phenol reagent, J. Biol. Chem. 193 (1951) 265–275.
[29] E.G. Bligh, W.J. Dyer, A rapid method of total lipid extraction and purification, Can. J. Biochem. Physiol. U. S. A. 37 (1959) 911–917.
[30] H. Schägger, G. von Jagow, Tricine-sodium dodecyl sulfate-polyacrylamide gel electrophoresis for the separation of proteins in the range from 1 to 100 kDa, Anal. Biochem. 166 (1987) 368–379.
[31] E. Goormaghtigh, V. Cabiaux, J.M. Ruysschaert, Determination of soluble and membrane protein structure by Fourier transform infrared spectroscopy: I. Assignments and model compounds, Sub-Cell. Biochem. 23 (1994) 329–362.
[32] X.M. Wang, R. Wattiez, M. Mock, P. Falmagne, J.M. Ruysschaert, V. Cabiaux, Structure and interaction of PA63 and EF (edema toxin) of *Bacillus anthracis* with lipid membrane, Biochemistry 36 (1997) 14906–14913.
[33] K.J. Rothschild, R. Sanches, N. Clark, Infrared absorption of photoreceptor and purple membranes, Methods Enzymol. 88 (1982) 696–714.
[34] M. Cortijo, A. Alonso, J.C. Gomez-Fernandez, Intrinsic protein–lipid interactions. Infrared spectroscopy studies of gramicidin A, bacteriorhodopsin and Ca^{2+}-ATPase in biomembranes and reconstituted systems, J. Mol. Biol. 157 (1982) 597–618.
[35] V. Cabiaux, R. Brasseur, R. Wattiez, P. Falmagne, J.M. Ruysschaert, E. Goormaghtigh, Secondary structure of diphtheria toxin and its fragments interacting with acidic liposomes studied by polarized infrared spectroscopy, J. Biol. Chem. 264 (1989) 4928–4938.
[36] H.H. de Jongh, E. Goormaghtigh, J.M. Ruysschaert, The different molar absorptivities of the secondary structure types in the amide I region: an attenuated total reflection infrared study on globular proteins, Anal. Biochem. 242 (1996) 95–103.
[37] C. Vigano, A. Margolles, H.W. van Veen, W.N. Konings, J.M. Ruysschaert, Secondary and tertiary structure changes of reconstituted LmrA induced by nucleotide binding or hydrolysis. A Fourier transform attenuated total reflection infrared spectroscopy and tryptophan fluorescence quenching analysis, J. Biol. Chem. 275 (2000) 10962–10967.
[38] H.H. de Jongh, E. Goormaghtigh, J.M. Ruysschaert, Tertiary stability of native and methionine-80 modified cytochrome *c* detected by proton-deuterium exchange using on-line Fourier transform infrared spectroscopy, Biochemistry 34 (1995) 172–179.
[39] V. Raussens, V. Narayanaswami, E. Goormaghtigh, J.M. Ruysschaert, Hydrogen/deuterium exchange kinetics of apolipophorin-III in lipid-free and phospholipid-bound states. An analysis by Fourier transform infrared spectroscopy, J. Biol. Chem. 271 (1996) 23089–23095.
[40] V. Cabiaux, E. Goormaghtigh, R. Wattiez, P. Falmagne, J.M. Ruysschaert, Secondary structure changes of diphtheria toxin interacting with asolectin liposomes: an infrared spectroscopy study, Biochimie 71 (1989) 153–158.
[41] E. Goormaghtigh, V. Cabiaux, J.M. Ruysschaert, Secondary structure and dosage of soluble and membrane proteins by attenuated total reflection Fourier transform infrared spectroscopy on hydrated films, Eur. J. Biochem. 193 (1990) 409–420.
[42] E. Goormaghtigh, J.M. Ruysschaert, in: R. Brasseur (Ed.), Molecular Description of Biological Membranes by Computer-Aided Conformational Analysis, CRC Press, Boca Raton, FL, 1990, pp. 285–329.
[43] E. Goormaghtigh, V. Raussens, J.M. Ruysschaert, Attenuated total reflection infrared spectroscopy of proteins and lipids in biological membranes, Biochim. Biophys. Acta 1422 (1999) 105–185.
[44] N. Challou, E. Goormaghtigh, V. Cabiaux, K. Conrath, J.M. Ruysschaert, Sequence and structure of the membrane-associated peptide of glycophorin A, Biochemistry 33 (1994) 6902–6910.
[45] H.H. de Jongh, E. Goormaghtigh, J.M. Ruysschaert, Monitoring structural stability of trypsin inhibitor at the submolecular level by amide–proton exchange using Fourier transform infrared spectroscopy: a test case for more general application, Biochemistry 36 (1997) 13593–13602.
[46] J.M. Zhao, E. London, Conformation and model membrane interactions of diphtheria toxin fragment A, J. Biol. Chem. 263 (1988) 15369–15377.
[47] K. Hammond, G.A. Caputo, E. London, Interaction of the membrane-inserted diphtheria toxin T domain with peptides and its possible implications for chaperone-like T domain behavior, Biochemistry 41 (2002) 3243–3253.
[48] P.O. Falnes, S. Olsnes, Cell-mediated reduction and incomplete membrane translocation of diphtheria toxin mutants with internal disulfides in the A fragment, J. Biol. Chem. 270 (1995) 20787–20793.
[49] L.K. Tamm, S.A. Tatulian, Infrared spectroscopy of proteins and peptides in lipid bilayers, the use and misuse of FTIR spectroscopy in the determination of protein structure, Q. Rev. Biophys. 30 (1997) 365–429.
[50] M. Jackson, H.H. Mantsch, Crit. Rev. Biochem. Mol. Biol. 30 (1995) 95–120.